Multidirectional curvilinear structures detection using steerable pyramid

Florence Denis*, Atilla Baskurt

LIRIS FRE 2672 CNRS / INSA de Lyon / Université Claude Bernard Lyon 1 / Université Lumière Lyon 2 / Ecole Centrale de Lyon,

Université Claude Bernard Lyon1, Bâtiment Nautibus, 8 boulevard Niels Bohr

69622 Villeurbanne Cedex, France

ABSTRACT

The work described in this paper concerns directional structures detection for particular aspects of inspection, such as scratches and marbling defect detection in leather images, or for particular medical imaging problems, such as mammography analysis. Because of the very specific geometry of these structures, we apply a multiscale and orientation-shiftable method. Scratches and marbling have various shapes and sizes. In mammograms, stellate masses have an irregular appearance and are frequently surrounded by a radiating pattern of linear spicules. Multiscale approaches using oriented filters have proved to be efficient to detect both types of curvilinear patterns.. The detection is based on steerable filters, which can be steered to any orientation fixed by the user, and are synthesized using a limited number of basic filters. These filters are used in a recursive multi-scale transform: the steerable pyramid. Then, the curvilinear structures are extracted from the directional images at different scales.

Keywords: multiscale decomposition, steerable filters, image analysis, curvilinear structures, defect detection, mammograms.

* fdenis@liris.cnrs.fr; phone +33 4 72 43 19 75; fax: +33 4 72 43 13 12

1. INTRODUCTION

The object of this work is directional structures detection for particular aspects of inspection or for medical imaging. The detection is based on steerable filters, which can be steered to any orientation fixed by the user, and are synthesized using a limited number of basis filters. These filters are used in a recursive multi-scale transform: the steerable pyramid. Using the steerable pyramid, oriented contrast enhancement can also be performed. In this study, we will focus on the detection of directional structures. We are also interested in the analysis of local orientations. Some structures such as stellate tumor in mammograms can be characterized with curvilinear structures in several directions. So, we develop an image analysis method based on a multiresolution approach using steerable filters. The steerable filters are directional derivative operators, which can vary in size and orientation, in a way to provide multiscale and multiresolution analysis. They can be recursively applied to successive high-pass band of the image resulting in a steerable pyramid decomposition [1]. The method is applied to extract both scratches and other defects from leather images and to stellate mass diagnosis in mammograms.

2. THE STEERABLE PYRAMID

Steerable filters: definition

Let $f(x,y)$ be a two-dimensional function. We call $f^{\theta}(x,y)$ the rotated version of f by a θ angle. Freeman and Adelson [2] define the property of steerability as follows:

> "f is called steerable if it can be written as a linear sum of rotated versions of itself ".

The steering constraint is then:

$$f^{\theta}(x,y) = \sum_{i=1}^{M} k_i(\theta).f^{\theta_i}(x,y) \qquad (1)$$

where $k_i(\theta)$ are the interpolation functions and M the number of basis images. The authors have also detailed the conditions under which f is steerable, the minimum number M of terms required and what $k_i(\theta)$ are.

The steerable pyramid: definition

The steerable pyramid uses steerable filters in a multiscale recursive scheme. This structure, proposed by Simoncelli and Freeman [1], is shown in Figure 1. Initially, the image is separated into low and high-pass subbands. The former is then divided into M oriented bandpass subbands and a lower-pass subband. This last one is then subsampled by a factor of 2, both in the x and y directions. The recursivity is achieved by inserting another level of decomposition in the lower branch.

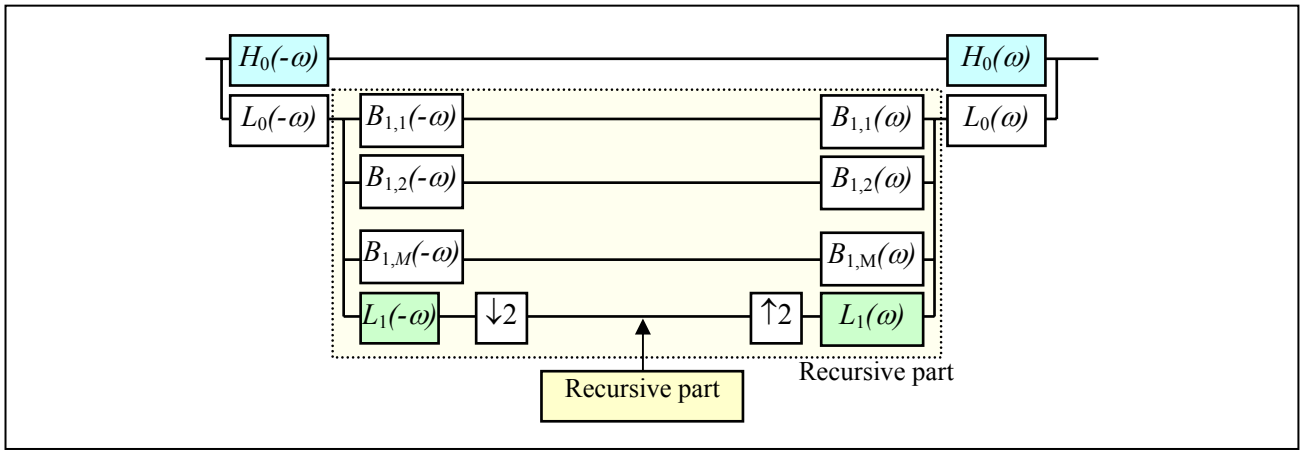

Figure 1: Decomposition scheme in the frequency domain

Figure 1 shows that the reconstructed image in the frequency domain is:

$$\hat{F}(\omega) = \left\{ |H_0(\omega)|^2 + |L_0(\omega)|^2 . |L_1(\omega)|^2 + \sum_{i=1}^{M} |B_{1,i}(\omega)|^2 \right\} . F(\omega) + a.t. \tag{2}$$

where *a.t.* are aliasing terms. For recursion, when a level $l+1$ is considered, the filters $B_{l+1,i}$ and L_{l+1} are defined by:

$$\begin{aligned} B_{l+1,i}(\omega) &= B_{l,i}(\frac{\omega}{2}) \qquad \text{where} \quad i = 1..M \\ L_{l+1}(\omega) &= L_l(\frac{\omega}{2}) \end{aligned} \tag{3}$$

This particular way of combining steerable filters brings new constraints, which are described by Karasaridis and Simoncelli [3]: first, the low-pass response at level l must remain the same when the $l+1^{th}$ level is added. Second, to perform a perfect reconstruction, we must on one hand insure the elimination of the aliasing terms (Shannon theorem) and on the other hand avoid amplitude distortion. Finally, the filters must be steerable (1). Those constraints imply three conditions on the radial part:

$$\begin{aligned} &L_1(\omega) = 0 \qquad \text{if} \qquad |\omega| > \frac{\pi}{2} \\ &|L_1(\omega)|^2 + \sum_{i=1}^{M} |B_{1,i}(\omega)|^2 = 1 \\ &|H_0(\omega)|^2 + |L_0(\omega)|^2 = 1 \end{aligned} \tag{4}$$

The oriented band-pass filters $B_{1,i}$ are built by combining a high-pass radial filter H_1 with an angular function $A_i(\theta)$:

$$B_{1,i}(\omega) = H_1(\omega).A_i(\theta) \quad \text{where} \quad \theta = \arg(\omega) \tag{5}$$

We use filters whose radial part is a constant unit response in the passing band and a raised-cosine falloff of one octave width, as shown in Figure 2, and whose angular part $A_i(\theta)$ is given by:

$$A_i(\theta) = \left[-j.\cos(\theta - \theta_i)\right]^{M-1} \qquad \text{where} \quad \theta = \arg(\omega), \ \theta_i = \frac{\pi(i-1)}{M} \text{ and } j^2 = -1 \tag{6}$$

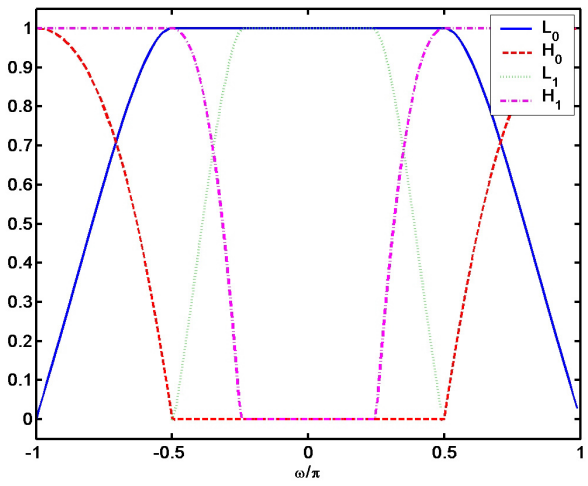

Figure 2 : radial profile for L_0, H_0, L_1 and H_1 filters

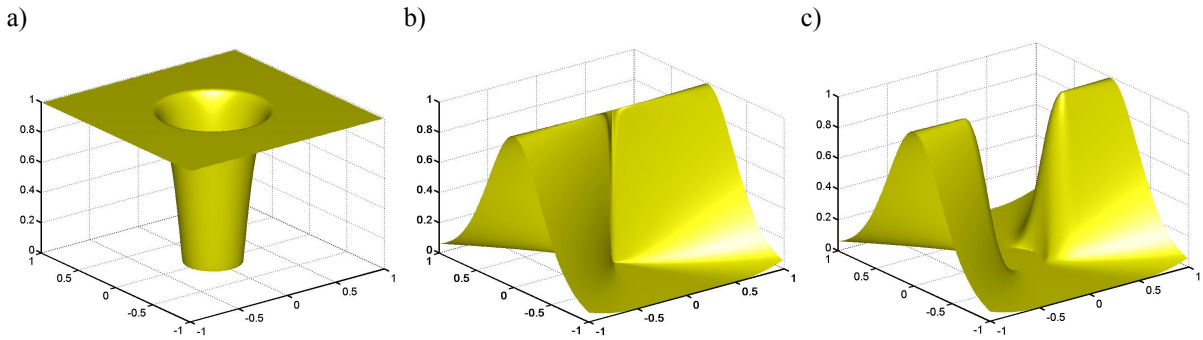

Figure 3 : a) high-pass filter $H_1(\omega)$,
b) angular part $A_1(\theta)$ for a 9 directions decomposition
c) resulting oriented band-pass filter $B_{1,1}(\omega)$

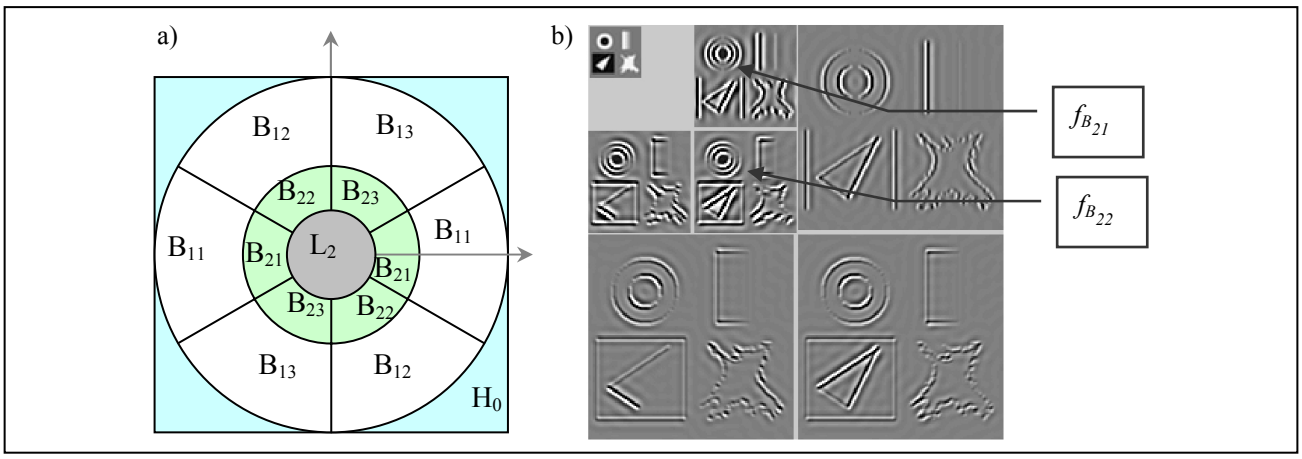

Figure 4: Filter cascade scheme for the steerable pyramid with M=3 and a two levels decomposition

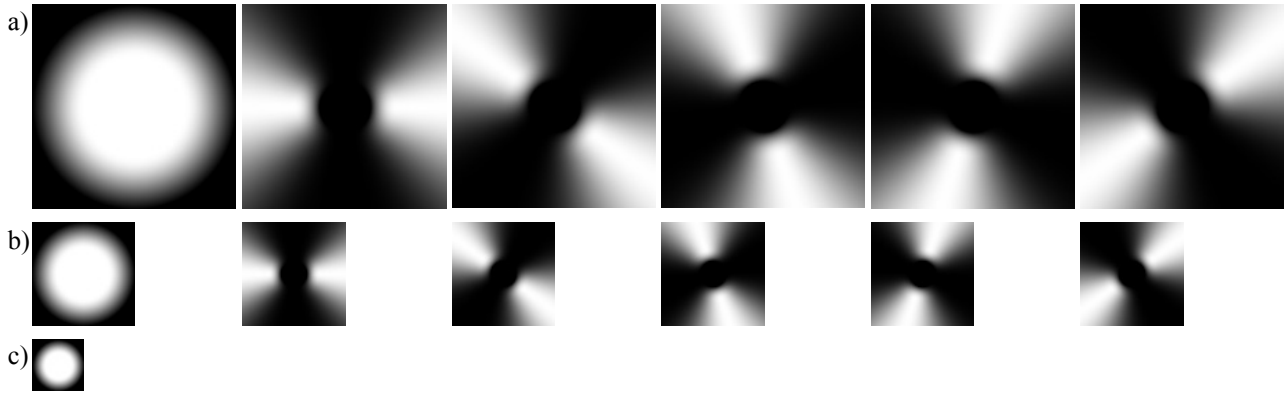

Figure 5: Magnitude of the filters frequency response for a two level decomposition with 5 directions

a) L_0, $B_{1,1}$ to $B_{1,5}$

b) L_1, $B_{2,1}$ to $B_{2,5}$

c) L_2

Figure 3 shows a particular oriented band-pass filter for $\theta_i = 0°$. An example of decomposition in the frequency domain is shown in Figure 4a. The figure shows how the frequency domain is partitioned in subbands with the steerable pyramid, using two scales and three orientations. Figure 4b shows the result images of a two-scale steerable pyramid transform with three orientations. The image $f_{B_{22}}$ corresponds to the content of the subband B_{22}. Figure 5 shows the filters for a two level decomposition with five directions.

1.1. Steerable pyramid versus other multiscale techniques

Steerable filters have been developed for early-vision problems of features extraction, while they give rise to a set of subbands of particular orientations. The use of these filters in a multiscale transform with the steerable pyramid contitutes a powerful tool for many aspects of image analysis. The steerable pyramid scheme is recursive and the transformation matrix is self-inverting: inverting the process consists in applying the inverse matrix of the transform. This is usually called a "tight frame". Its other main advantages are translation invariance and rotation invariance, which are of great benefit for image fusion [4], texture characterization [5, 6], contrast enhancement [7] or noise removal [8].

Multiscale techniques are generally compared to wavelets. Wavelet transform are also recursive and self-inverting but not always rotation-invariant and translation-invariant. Yet, unlike wavelets, the steerable pyramid decomposition is over-complete: it takes more memory space than the original image. The rate between the two is *1+4M/3*. Therefore, the steerable pyramid is more adapted to image analysis than to image compression.

Another tool for multidirectional image analysis has been developed by Candès[9] with ridgelets, which are defined from 1D wavelet function along one direction and constant function along the other axis. This transform is effective only for straight lines detection. For more complex images presenting curvilinear structures, the ridgelets have to be applied locally after a block decomposition leading to a curvelet type analysis [10]. This usually generates discontinuities on the whole curvilinear structure detected.

Among other multidirectional image analysis techniques Gabor filter banks have interesting properties of localization in spatial and frequency domain, and can be continuously tuned to arbitrary directions and bandwidths. But unlike the steerable pyramid, they don't allow a complete and uniform coverage of the frequency domain, so they provide an analysis tool but does not allow reconstruction.

3. DIRECTIONAL STRUCTURES DETECTION USING THE STEERABLE PYRAMID

A non linear image enhancement method has been proposed by Wu, Schulze and Castleman [7] which enables a selective enhancement, at a chosen scale l, in a chosen direction θ. The principle is as follows: since they wish to enhance, the "black-white-black" transitions in the image, they keep only the negative part of the filtered response along the θ direction, which they subtract, with an adjustable strength from the image at the current level, to obtain the enhanced image.

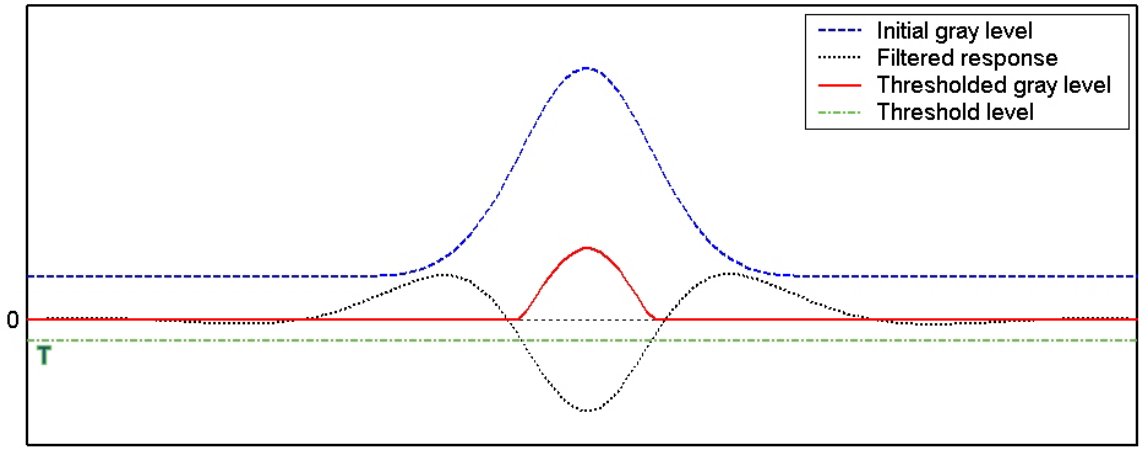

Figure 6: One dimensional illustration of the detection method for a white-black-white transition (blue dashed line) The black dotted line depicts the filter response and the red solid line shows the negative part of this response after thresholding

In order to detect directional structures, we propose to use this negative part of the filtered response, and, to have bright positive response on a dark background, we take the opposite of the thresholded response. Let us call θ_i the direction in which we intend to analyze the image at a given level l. $f_{B_{l,i}}$ denotes the image filtered in direction θ_i with $B_{l,i}$ (Figure 4). We consider the thresholded image:

$$\begin{aligned} f^{-}_{B_{l,i}}(x,y) &= -f_{B_{l,i}}(x,y) \quad \text{if} \quad f_{B_{l,i}}(x,y) < 0 \\ f^{-}_{B_{l,i}}(x,y) &= 0 \quad \text{if} \quad f_{B_{l,i}}(x,y) \geq 0 \end{aligned} \tag{7}$$

Indeed, the thresholded components are precisely aligned with the "black-white-black" lines.

Figure 6 shows a one-dimensional example with both the reconstructed signal, the filtered signal and the thresholded and inverted signal.

Other types of defect, i.e. “white-black-white” transitions can be found keeping only the positive part of the response instead of the negative one. Moreover, a non-zero threshold *T* allows to control the strength of transitions that will be detected, and to filter out noisy components, such that (6) becomes:

$$\begin{cases} f^{-}_{B_{l,i}}(x,y) = T - f_{B_{l,i}}(x,y) & \text{if} \quad f_{B_{l,i}}(x,y) < T \\ f^{-}_{B_{l,i}}(x,y) = 0 & \text{if} \quad f_{B_{l,i}}(x,y) \geq T \end{cases}$$
$$\begin{cases} f^{+}_{B_{l,i}}(x,y) = f_{B_{l,i}}(x,y) - T & \text{if} \quad f_{B_{l,i}}(x,y) > T \\ f^{+}_{B_{l,i}}(x,y) = 0 & \text{if} \quad f_{B_{l,i}}(x,y) \leq T \end{cases} \tag{8}$$

where $f^{-}_{B_{l,i}}(x,y)$ denotes the thresholded image for "black-white-black" detection and $f^{+}_{B_{l,i}}(x,y)$ for “white-black-white” detection.

So depending on what kind of threshold is set on the response we can detect and analyze different kinds of stuctures. The threshold level can be adjusted from 0 to the maximal level value allowing to remove textured background for example. It has to be set by the user according to the image characteristics and the structures which have to be extracted.

Thresholding is performed for each direction and a resulting image is built by taking, at each point, the maximum value of those obtained for all directions:

$$f^{max}_{B_l}(x,y) = \max_i \left\{ f^{\pm}_{B_{l,i}}(x,y) \right\} \tag{9}$$

Then, the process is pursued with lower levels, till level l is reached, resulting in L maximum images. All the thresholded directional images can also be saved and analyzed. Indeed, the local energy patterns obtained, at each level, for small blocks, from the energy of all the filtered and thresholded images can be of great interest, to determine, for example, the defect major direction or crossings, etc.

The thresholded image can also be used, at each step for image enhancement. The enhanced image is computed by:

$$\begin{cases} f^{e}_{B_{l,i}} = f_{B_{l,i}}(x,y) - \eta_l \cdot f^{-}_{B_{l,i}}(x,y) & \text{for "white - black - white" enhancement} \\ f^{e}_{B_{l,i}} = f_{B_{l,i}}(x,y) + \eta_l f^{+}_{B_{l,i}}(x,y) & \text{for "black - white - black" enhancement} \end{cases} \quad (10)$$

where η_l is chosen by the user, and controls the strength of the enhancement at a given level *l*. It may vary from one level to another depending on the size of details to enhance.

The enhancement is performed for each level and each direction and a resulting image is built by taking, at each point, the minimum ("white-black-white" enhancement) or maximum ("black-white-black" enhancement) value of those obtained for all directions:

$$\begin{cases} f^{e}_{B_l}(x,y) = max_i \left\{ f^{e}_{B_{l,i}}(x,y) \right\} & \text{for "white - black - white" enhancement} \\ f^{e}_{B_l}(x,y) = min_i \left\{ f^{e}_{B_{l,i}}(x,y) \right\} & \text{for "black - white - black" enhancement} \end{cases} \quad (11)$$

After enhancement at all levels, the reconstruction is pursued using the enhanced images.

It becomes now evident that the steerable pyramid is a powerful tool to analyze, quantify and selectively enhance directional structures in images:

- the steerability property allows to determine precisely the direction;
- the multiresolution aspect gives rise to structure size knowledge;
- the threshold process allows to select between different types of transitions.

Let's note, however, that a precise angular detection is possible only if the angular coverage of each oriented subband is narrow, i.e. if the number of orientations is large enough.

4. DEFECT CHARACTERIZATION

The steerable pyramid has been applied to leather images where the manufacturer wants to detect various defects such as scratches and marbling, their directions, their size and their crossings if any. These images show a textured and noisy background which can be spoiled by curvilinear defects, either darker or lighter than the background. Figure 7 shows three examples of such defects.

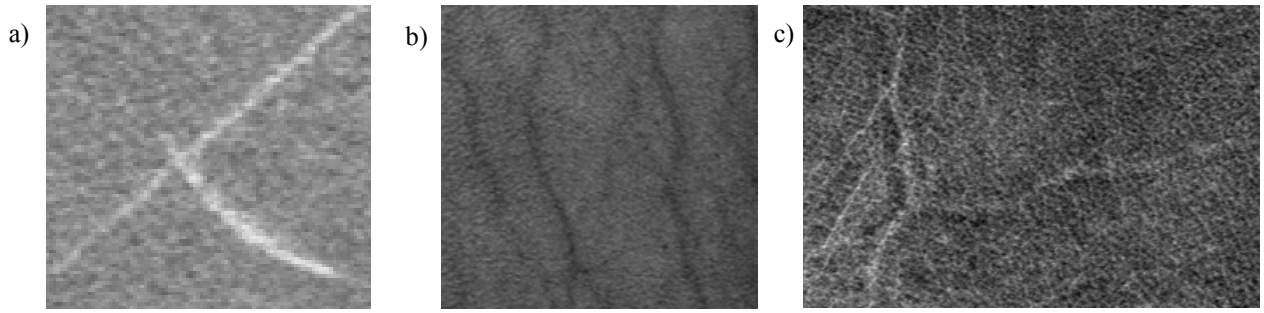

Figure 7: Three examples of leather images

To achieve good angular selectivity, the number of directions has been fixed to 9, which corresponds to a 20 degrees angle. Figure 8 shows the directional images $f_{\bar{B}_{2,i}}(x,y)$ and $f_{\bar{B}_{3,i}}(x,y)$ after thresholding for level 2 and 3 of a 9 directions decomposition, for a "black-white-black" detection. The two defects of Figure 7a are isolated in the direction images 3-4 and 7-8. It is important to detect separately different defects in order to analyze their own aspect. Figure 9a presents the resulting image $f_{B_2}^{max}(x,y)$ obtained from 9 directional images of level 2. Each pixel represents the maximum value between 9 pixels issued from Figure 8a. This image synthesizes the information for level 2. Little lines appear apart from the scratches, due to the image background texture. The gray level of these lines is very low compared to the defect gray level so that they can be removed by further thresholding (see Figure 11a-c) or by setting a non-zero threshold T (see equation 7).

Same comments concern Figure 9b which resumes the level 3 activity. Figure 10 illustrates a “white-black-white” detection with Figure 7b and a "black-white-black" with Figure 7c. Non-zero thresholds have been set to remove textured components. Figure 11e and Figure 11f present the binary images obtained from Figure 10. It can be noted that the defects are completely detected in the presence of a noisy background. For a comparison, Figure 12 shows the images obtained after a Laplacian of Gaussian filter: the textured background remains and can not be removed with further thresholding.

A set of 9 images with various defects have been studied and for all a satisfying detection has been obtained, considering the very low contrast of defects compared the textured background.

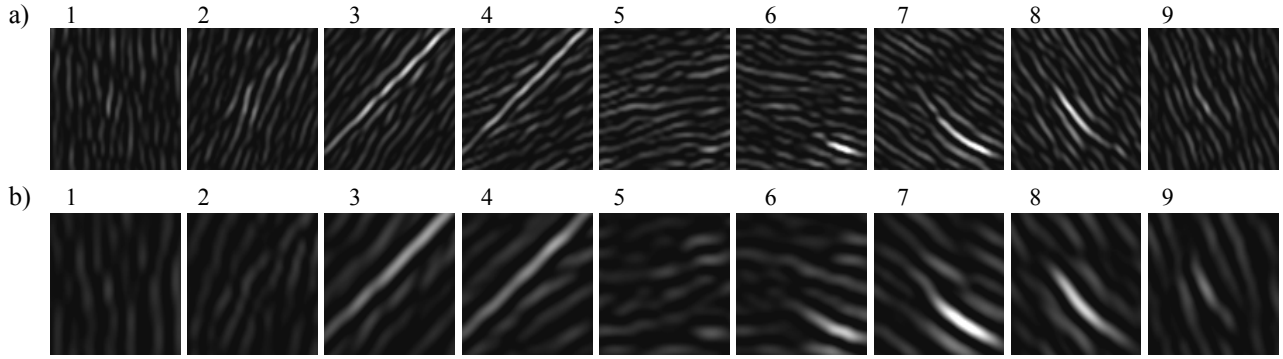

Figure 8: thresholded directional images with zero threshold for the image depicted on Figure 7a for 9 directions

a) $f_{\bar{B}_{2,1}}(x,y)$ to $f_{\bar{B}_{2,9}}(x,y)$

b) $f_{\bar{B}_{3,1}}(x,y)$ to $f_{\bar{B}_{3,9}}(x,y)$

Figure 9: Maximal images for the image depicted on Figure 7a

a) $f_{B_2}^{max}(x,y)$

b) $f_{B_3}^{max}(x,y)$

a) b)

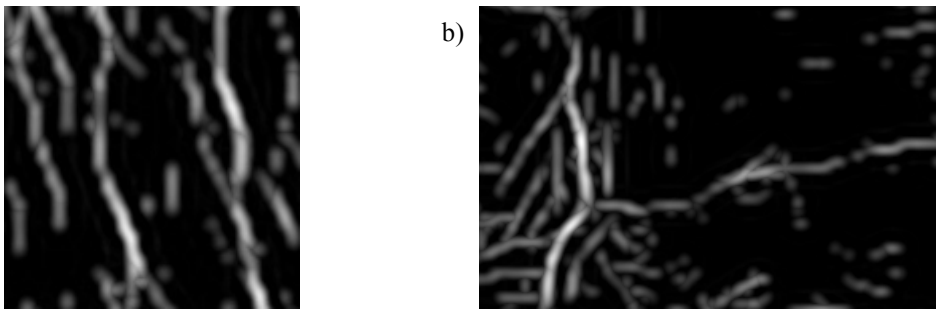

Figure 10 : Maximal image $f_{B_3}^{max}(x, y)$

a) for the image depicted on Figure 7b at level 3 for 9 directions with a threshold T=22
b) for the image depicted on Figure 7c at level 3 for 9 directions with a threshold T=30

a) b) c) d)

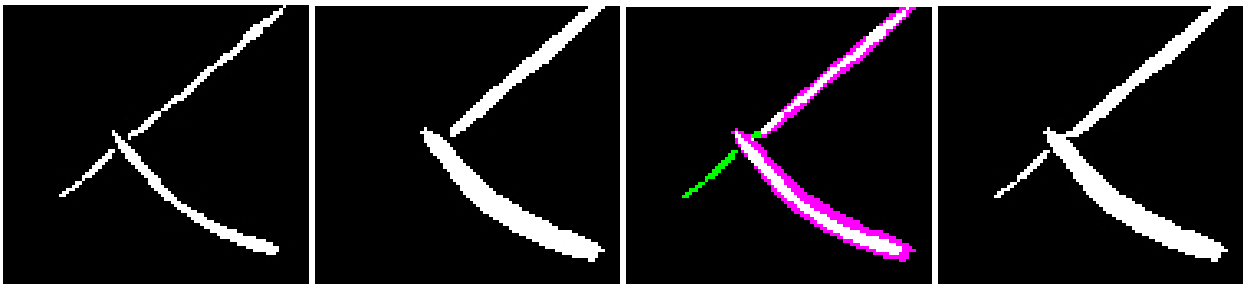

e) f)

Figure 11: Resulting images

a) after thresholding for the image depicted on Figure 9a

b) after thresholding for the image depicted on Figure 9b

c) superposition of images a) and b) :

green : white pixels in a) only

magenta : white pixels in b) only,

white : white pixels in a) and b)

d) maximal image obtained from a) and b) (logical OR)

e) binary image obtained from Figure 10 a

f) binary image obtained from Figure 10 b

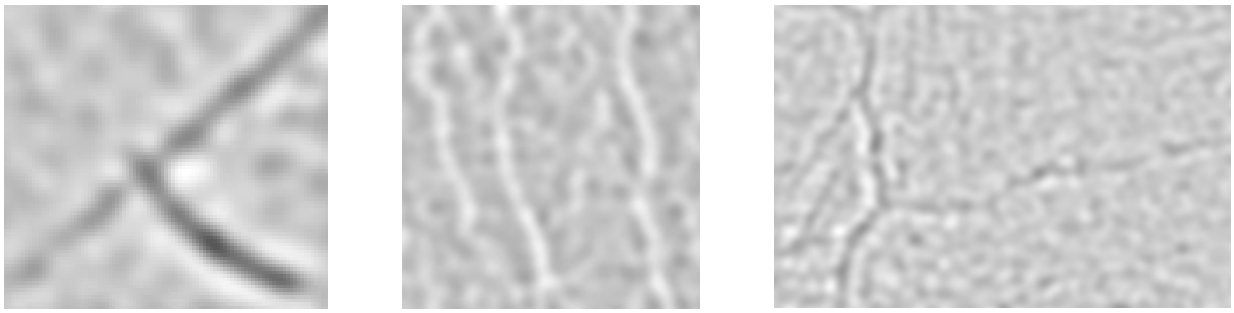

Figure 12: Resulting images for a Laplacian of Gaussian filter
a) for the image depicted on Figure 7a
b) for the image depicted on Figure 7b
c) for the image depicted on Figure 7c

5. STELLATE MASS DETECTION

Breast cancer is currently among the leading causes of death for middle-aged women world-wide. For example, every year, 26000 new cases are detected in France and 9000 women die from cancer. The early diagnosis and detection of breast cancer is the key to its successful management. X-ray mammography is the recommended method for early detection and identification of subtle, minute microcalcifications and other signs of abnormalities on X-ray mammograms can assist in the early diagnosis of non-palpable breast carcinoma. However, radiologists cannot detect all incipient stages of cancer that are visible in follow-up examinations of mammographic images. It has been estimated that 30% or more of potentially detectable lesions are missed. In addition, only 10 to 35% of detected lesions that are sent for biopsy are found to be cancerous. Once in the digital domain (scanned mammograms), the processing power of the computer can be applied to assist in the diagnostic process. The form (nodular or stellate masses), the volume, the lesion homogeneity, the presence or absence of microcalcifications are informations that can be extracted from these images, in order to increase the diagnostic accuracy of mammography screening programs. Mass abnormalities can be classified into three main categories: stellate (or spiculated), ill-defined and well-defined masses. The different properties of these tumors, as well as the complex background in the mammogram, make it difficult for one algorithm to work efficiently. Furthermore,

normal breast tissue often looks like tumors. Many studies have focused on this issue: "how to distinguish pathologic tissues from normal ones?" and several different approaches have been proposed. Most of them include an enhancement pre-processing, a detection scheme and a classification algorithm. More details can be found in [11,12] In this study, we focus on the detection of stellate masses which present a geometric form and also privileged directionality.

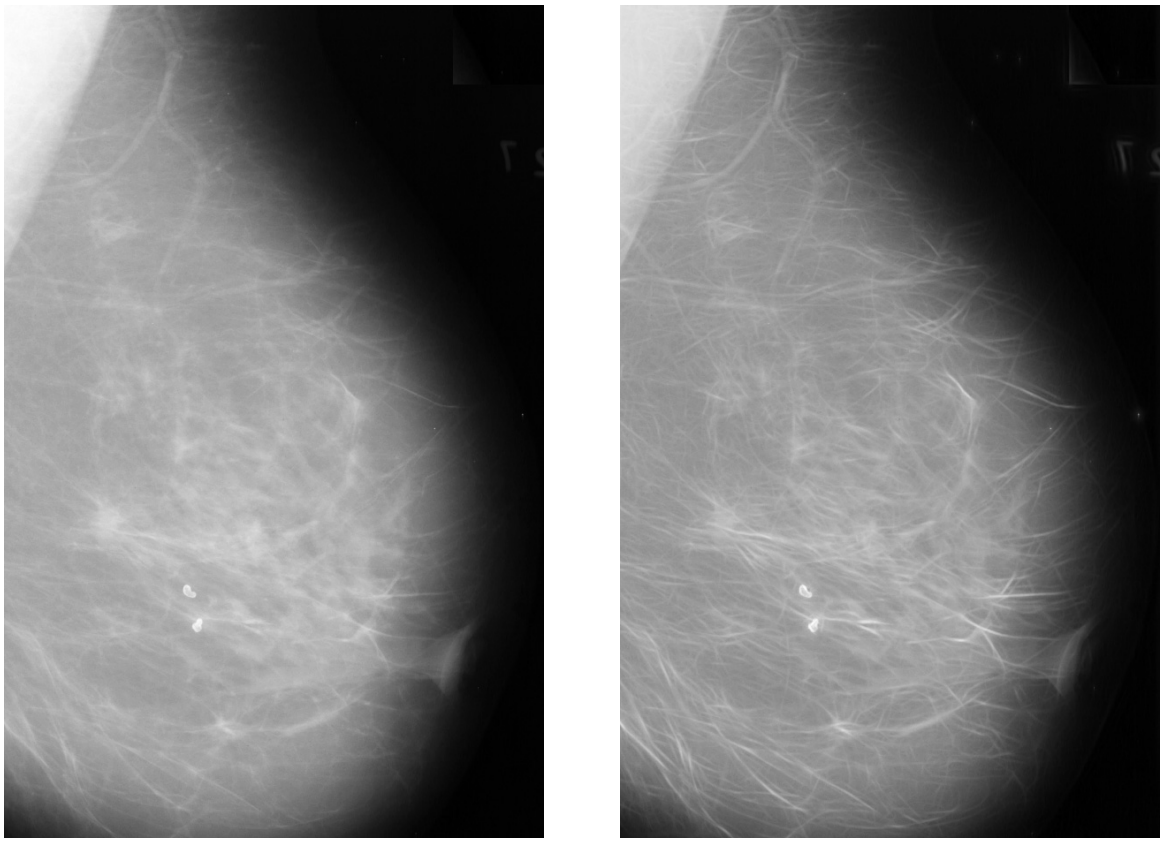

Figure 13 : a) original mammographic image
b) enhanced image using a zero threshold and η_1 =4 for level 1, η_2 =2 for level 2 and η_3 = 1 for level 3

The proposed method, when applied for stellate mass detection uses the same principle as for defect detection. Moreover, to help the radiographer during the final diagnosis step, the images are also enhanced to reveal “black- white – black” transitions. Figure 13 shows an example of results obtained for enhancement at level 2 and 3, where the contrast is clearly improved. Indeed, the enhancement technique, which considers the maximal value for each image pixel, does not reveal stellate patterns with many

characteristic directions. Then, the directional information has to be pointed out for the decision step. The selection of suspicious regions is based on the following considerations:

- stellate opacities are slightly bright structures compared to the surrounding breast tissues;
- they have stellate morphology with fibrous branches in several directions.

So, the detection process will act in two steps, first detecting the curvilinear structures for each direction and then deciding if these structures correspond to suspicious tissues or only normal ones. The later step uses the thresholded images for each direction, from which energy values are computed over small blocks. A moving window is considered whose size has to chosen large enough to contain several direction branches when a stellate mass is present and yet small enough to insure local information. For each position of this moving window in the image plane, all directional images are considered for each level and their local energy over the moving window are computed. At each level, from these energy values for all directions, energy patterns centered in the moving window can be drawn, whose shape is related to the image content. If a stellate mass is present, radial branches appear in several directions and the energy pattern exhibits high isotropy. At the opposite, for normal tissues, only few directions are found (the inherent structure of breast tissue) and the energy pattern is very anisotropic. Figure 14 shows an example of curvilinear structures detection and the corresponding energy patterns at level 2 and 3. For shape comparison, all the patterns sizes have been normalized to have the same maximal angular value. The colors of the patterns are related to their normalized area i.e. the area computed after the size normalization. Values about one (red patterns) indicate isotropic patterns, close to circles, while small values (blue patterns) correspond to highly anisotropic ones. One can remark that red patterns clearly appear on the pathological zone while all the others are blue or yellow. Level 2 shows some orange and red patterns on other areas, corresponding to superposition of mammographic curvilinear structures, but they disappear at level 3, so that they can be distinguished from stellate masses. Note that the goal is not to automatically detect the presence of a tumour and to identify its category. These results are to be analyzed by the experts in order to indicate them that there are some spatial locations in a mammogram with potential presence of tumour.

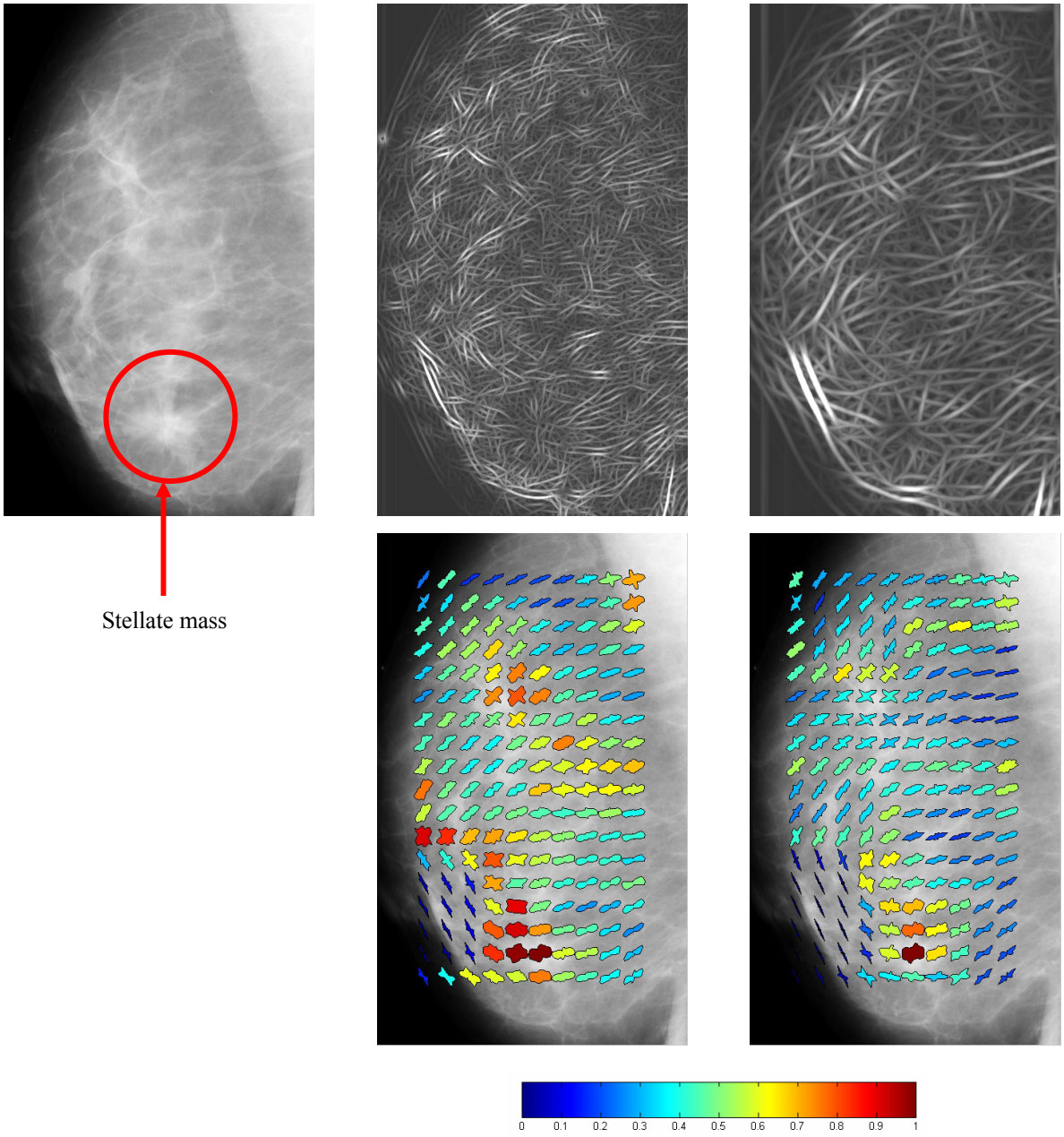

Figure 14 : results of stellate mass detection for a mammographic image

a) original image (size : 425x700 pixels)

b) and c) maximal images $f_{B_2}^{max}(x,y)$ and $f_{B_3}^{max}(x,y)$

d) and e) energy patterns at level 2 and 3 computed on windows of 128x128 pixels with 32 pixels increments in window positions

The method has been applied on 25 breast images with stellate masses, giving interesting results. But, due to the very high variablility of mammographic images, the low level of contrast of some images and the presence of many curvilinear structures that can hide stellate masse, it sometimes fail in finding tumours. Normal tissues, with curvilinear structures in many directions are also detected resulting in false alarms. To overcome these problems, improvements are under development.

CONCLUSION

A method for directional structure detection has been proposed. It is based on the steerable pyramid decomposition and reconstruction scheme. During the reconstruction, the pixels of one directional image at a given scale are processed according to a user threshold to select either dark or light lines and eliminate noise. Using these images, the directional structures are extracted or enhanced. The method is applied to scratches and marbling detection in leather images, and it shows encouraging results, since different types of defects have been isolated from various textured backgrounds. An other development concerns stellate mass detection in mammograms. Our radiologists, expert for mammograms, visually analyzed the preliminary results obtained and thought that this tool can really help the early diagnosis and detection of stellate masses. The proposed method is a generic approach which can be easily adapted to other imaging modalities and different kinds of industrial defects or of medical problems. The generalization of the method to 3D images is under investigation.

BIBLIOGRAPHY

1. Simoncelli E. P., Freeman W. T., “The Steerable Pyramid: A Flexible Architecture for Multi-Scale Derivative Computation”, *IEEE Second Int'l Conf on Image Processing*, Washington DC, Vol. III, pp. 444-447, IEEE Sig Proc Society, October 1995.

2. Freeman W., Adelson E., “The Design and use of Steerable Filters”, IEEE Trans. pattern anal. machine intel., **Vol. 13**, pp 891-906, Sept. 1991.

3. Karasaridis A., Simoncelli E., “A Filter Design Technique for Steerable Pyramid Image Transforms”, *Proc. IEEE ICASSP*,Vol. IV, pp. 2389-2392, IEEE Sig Proc Society, May 1996.

4. Liu Z., Tsukada K., Hanasaki K., Ho Y.K., Dai Y.P.,”Image fusion by using steerable pyramid”, *Pattern Recognition Letters,* **Vol. 22**, pp929-939, 2001

5. Simoncelli E., Portilla J., “Texture characterization via joint statistics of wavelet coefficient magnitudes”, *Fifth IEEE Int'l Conf on Image Proc*, Vol. I, Chicago, October 4-7, 1998.

6. Heeger D., Bergen J., “Pyramid based texture analysis/synthesis”, Computer Graphics, pp. 229-238, SIGGRAPH 95, 1995

7. Wu Q., Schulze M. A., Castleman K. R., “Steerable Pyramid filters for Selective Image enhancement applications”, *Proc. IEEE ISCAS*, Paper 1838, Session WAA2-2, 1998.

8. Simoncelli E. P., Adelson E. H., “Noise removal via Bayesian wavelet coring”, *IEEE Int. Conf. on Image Proc. ICIP 1996,* (Switzerland), September 1996.

9. Candès E. J., “Ridgelets : theory and applications” *Ph.D. thesis*, Department of statistics, Stanford University, 1998.

10. Candès E. J., Donoho D. L., “Curvelets – a surprisingly effective non adaptive representation for objects with edges”, *Curve and Surface fitting,* A. Cohen, C. Rabut and L. L. Schumaker, Eds., Saint-Malo, 1999, Vanderbilt University Press.

11. Morrow W.M., Paranjape R.B., Rangayyan R.M., Desautels J.E.L., “Region-based contrast enhancement of mammograms”, IEEE Transactions on Medical Imaging, **Vol. 11**, no. 3, pp. 392-406, Sept. 1992.

12. Mudigonda N. R.,Rangayyan R. M., Desautels J. E. L., “Gradient and texture analysis for the classification of mammographic masses”, IEEE trans. on medical imaging, **Vol. 19**, no. 10, pp. 1032-1043, Oct. 2000.

Dr. Florence DENIS was born in Marseille, France, in 1962. She received the B.S. degree in 1985, the M.S. in 1985 and the PhD in 1990 from the INSA-Lyon Scientific and Technical University, France. Since 1990, she works as associate professor at the University of Lyon. She is currently member of the image processing group at the LIRIS Laboratory. Her research interests are in the fields of 2D and 3D image processing, segmentation and watermarking.

Dr. A. Baskurt was born in Ankara, Turkey in 1960. He received the B.S. degree in 1984, the M.S. in 1985 and the Ph.D. in 1989, all in electrical engineering from INSA of Lyon, France. From 1989 to 1998, he was "Maître de Conférences" at INSA of Lyon. Since 1998, he has been with the University Claude Bernard of Lyon, France, where he is a Professor in Electrical and Computer Engineering. Dr. A. Baskurt leads the Images & Videos Group of LIRIS research laboratory at this University. This group performs image and video analysis and segmentation for image compression, image retrieval and shape detection and identification. His technical research and experience includes digital image processing, image compression and segmentation, image indexing and retrieval, especially for multimedia applications.